Nuclear Physics B359 (1991) 283–300
North-Holland

RADIATIVE CORRECTIONS TO HIGGS BOSON PRODUCTION*

S. DAWSON

Physics Department, Brookhaven National Laboratory, Upton, NY 11973, USA

Received 28 November 1990
(Revised 14 February 1991)

We calculate the $O(\alpha_s^3)$ radiative corrections to Higgs boson production in hadronic colliders in the infinite top-quark mass limit. Our calculation is valid for energy scales and Higgs boson masses which are much less than the top-quark mass. The contributions from the $gg \to HX$, $q\bar{q} \to H$, $qg \to qH$ and $\bar{q}g \to \bar{q}H$ subprocesses are included.

1. Introduction

One of the last remaining puzzles of the standard model of electroweak interactions is the existence of the Higgs boson. Although a single neutral scalar Higgs boson is required in the minimal standard model to give the W and Z gauge bosons their masses, the model gives no clue as to the mass of the Higgs boson. Experimentally, all that is known is that $M_H \gtrsim 40$ GeV [1]. A primary goal of all new accelerators is to search for the Higgs boson and either discover it or definitively exclude it over as large a mass region as possible.

High-energy hadron colliders such as the SSC and the LHC can search for a Higgs boson with a mass almost up to a TeV. The primary production mechanisms are gluon fusion, which is sensitive to the top-quark mass, and vector boson fusion. For $M_{top} \gtrsim 100$ GeV, the gluon fusion mechanism is dominant at the SSC for Higgs bosons lighter than about 700 GeV.

Special attention has been paid to the so-called "intermediate mass" Higgs boson. This is a Higgs boson with $40\ \text{GeV} \lesssim M_H \lesssim 2M_W$. In this region the Higgs boson cannot decay to W^+W^- pairs or to $t\bar{t}$ pairs. Hence the Higgs boson will decay predominantly to $b\bar{b}$ pairs. Since it is generally believed that it will be impossible to extricate the Higgs signal from $H \to b\bar{b}$ from the enormous QCD background, attention has focused on the rare decay modes of the Higgs boson in this region. These rare modes, such as $H \to \gamma\gamma$ or $H \to Ze^+e^-$, have branching ratios between 10^{-3} and 10^{-5} and so the number of expected events is quite small.

* Supported by the US Department of Energy under contract DE-AC02-76CH00016.

Elsevier Science Publishers B.V. (North-Holland)

It will therefore be extremely difficult to see an intermediate mass Higgs boson and so it is important to be able to predict its production rate as reliably as possible.

In this paper we compute the radiative corrections of $O(\alpha_s^3)$ to Higgs boson production in hadronic collisions. These include the virtual contributions to the lowest-order process $gg \to H$ as well as real gluon emission, $gg \to gH$, and also the processes $q\bar{q} \to gH$ and $q(\bar{q})g \to q(\bar{q})H$. We obtain the leading corrections in the limit $M_{top} \to \infty$ and use them to compute Higgs boson production rates. Our results are valid in the limit $M_{top} \gg M_H$ and $M_{top} \gg \sqrt{s}$, and so should be a reliable estimate for the intermediate mass Higgs boson. The $O(\alpha_s^3)$ corrections have also been computed by Djouadi et al. [2] and we compare our results with theirs.

In sect. 2, we review the lowest-order results for the gluon fusion subprocess. We also compare the gluon fusion subprocess with the alternate production mechanism, vector boson fusion, and discuss the relative importance of the two mechanisms for different top-quark masses. In sect. 3 we present the $O(\alpha_s^3)$ contribution to Higgs production. Numerical results for $pp \to H$ at the SSC ($\sqrt{S} = 40$ TeV) and the LHC ($\sqrt{S} = 17$ TeV) are given in sect. 4. Finally, sect. 5 contains some conclusions.

2. Lowest-order results

The lowest-order amplitude for the gluon fusion of a Higgs boson arises from the triangle diagram of fig. 1. The amplitude is sensitive to all of the quarks which can couple to the gluon and to the Higgs boson, but has the property that it primarily depends on the heaviest quark mass (in practice, on the top-quark mass). The cross section has been available in the literature for some time [3],

$$\sigma_0(gg \to H) = \frac{\alpha_s^2}{\pi} \frac{M_H^2}{256v^2} |A|^2 \delta(s - M_H^2), \tag{2.1}$$

where

$$|A|^2 \equiv \left| \sum_q \tau_q \left(1 + (1 - \tau_q) f(\tau_q)\right) \right|^2 . \tag{2.2}$$

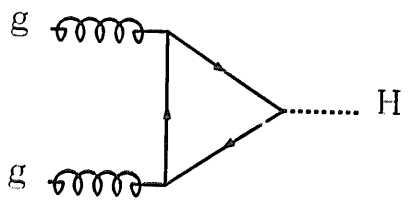

Fig. 1. Triangle diagram for $gg \to H$. The internal fermion lines include all quarks.

In eq. (2.2) the sum runs over all quarks with mass M_q, $v^2 = (\sqrt{2}\, G_F)^{-1} = 246$ GeV, $\tau_q \equiv 4M_q^2/M_H^2$,

$$f(\tau_q) = \begin{cases} \left[\sin^{-1}\left(\sqrt{1/\tau_q}\right)\right]^2 & \text{if } \tau_q \geqslant 1 \\ -\frac{1}{4}\left[\log(\eta_+/\eta_-) - i\pi\right]^2 & \text{if } \tau_q < 1 \end{cases}, \tag{2.3}$$

$$\eta_\pm \equiv 1 \pm \sqrt{1-\tau_q}\,. \tag{2.4}$$

In the limit that the quark mass is infinitely large, $\tau_q \to \infty$, $A \to \frac{2}{3}$ and

$$\sigma_0(gg \to H) \to \frac{\alpha_s^2}{\pi}\frac{M_H^2}{576v^2}\delta(s - M_H^2)\,. \tag{2.5}$$

In this paper we will consider only one heavy quark, the top quark, although we have in mind either the top quark or any new heavy fourth-generation quark.

When the momentum transfer to the Higgs boson is small, or equivalently in the limit $M_{top} \gg M_H$, the cross section to $O(\alpha_s^3)$ for $gg \to H$ can be obtained from the effective lagrangian [4]

$$\mathscr{L}_{eff} = -\frac{1}{4}\left(1 - \frac{\alpha_s}{3\pi v}H\right)G^{\mu\nu}G_{\mu\nu}\left(\frac{4\pi}{M_{top}^2}\right)^{\epsilon}\Gamma(1+\epsilon)\,, \tag{2.6}$$

where $G_{\mu\nu}$ is the gluon field strength tensor. It is straightforward to use eq. (2.6) to obtain the cross section of eq. (2.5) in $N = 4 - 2\epsilon$ dimensions and to include the $O(\epsilon)$ terms*,

$$\sigma_0(gg \to H) \to \frac{\alpha_s^2}{\pi}\frac{M_H^2}{576v^2}\left(\frac{4\pi}{M_{top}^2}\right)^{\epsilon}\Gamma(1+\epsilon)\delta(s - M_H^2)(1+\epsilon)\,. \tag{2.7}$$

In fig. 2, we analyze the validity of the infinite fermion mass limit by plotting the cross section for Higgs boson production via the gluon fusion subprocess for a variety of Higgs boson masses and comparing with the infinite quark mass limit. We see that when $M_H/M_{top} \lesssim 2$ the infinite fermion mass limit agrees within a factor of two with the exact calculation. In addition, the $M_{top} \to \infty$ limit always *underestimates* the cross section, so the results obtained in this manner are conservative.

The Higgs boson can also be produced from vector boson fusion [5],

$$q\bar{q}' \to W^+W^-X \to HX\,, \qquad q\bar{q} \to ZZX \to HX\,. \tag{2.8}$$

* Note that we must average over $4(1-\epsilon)^2$ transverse polarizations of the gluon–gluon initial state.

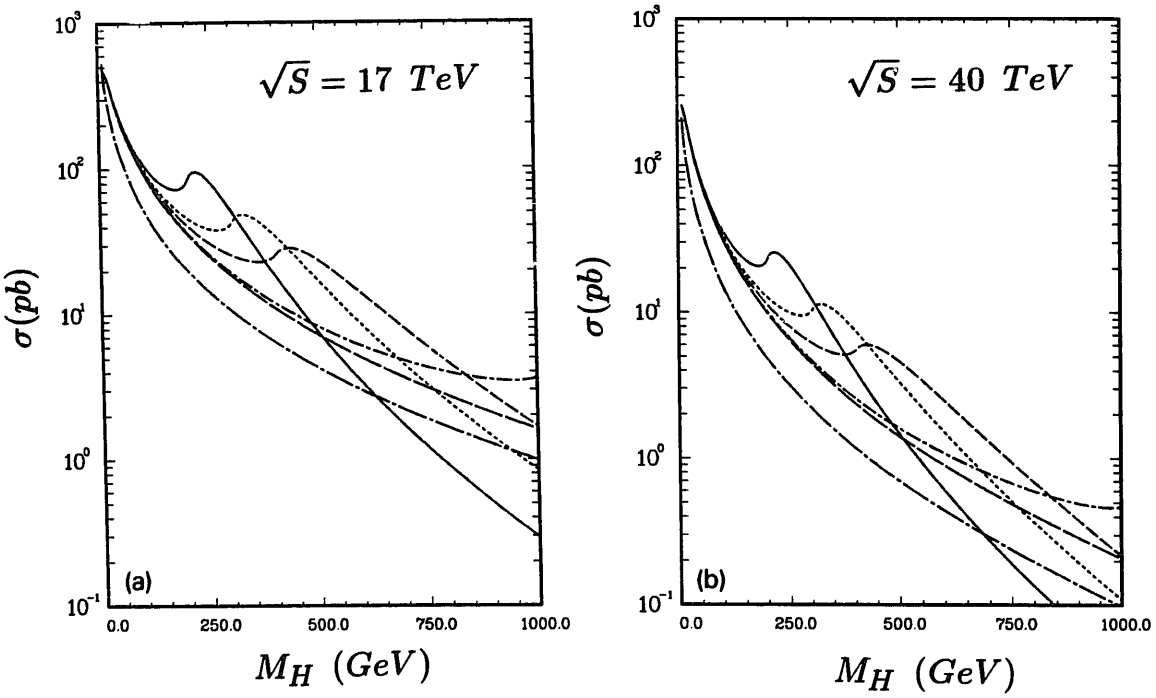

Fig. 2. Cross sections for pp → H through the gluon fusion subprocess at (a) $\sqrt{S} = 17$ TeV and (b) $\sqrt{S} = 40$ TeV. The solid, dotted, dashed and short-dash–dotted curves use the exact result for the cross section with $M_{top} = 100$, 150, 200 and 500 GeV, respectively, while the long-dashed curve is the result of the infinite quark mass limit of eq. (2.5). This figure includes only the lowest-order result. The long-dash–dotted line is the contribution to pp → H through the vector boson subprocess.

This mechanism is of course independent of the top-quark mass. For comparison, we show in fig. 2 the cross section for Higgs production from vector boson fusion at both the SSC and the LHC. We see that for $M_{top} \sim 200$ GeV, gluon fusion dominates for all values of the Higgs boson mass less than about 1 TeV, while for $M_{top} \sim 100$ GeV, gluon fusion dominates only for $M_H \lesssim 700$ GeV at the SSC. At the SSC, for $M_H \lesssim 250$ GeV, the contribution from vector boson fusion is always smaller than that from gluon fusion regardless of the top-quark mass. (Similar conclusions hold for the LHC.) In order to predict production rates, one must of course add the contributions from all production mechanisms. From fig. 2, it is clear that both gluon fusion and vector boson fusion are numerically important. In this paper we focus entirely on obtaining the best predictions for the gluon fusion contribution to Higgs boson production; the $O(\alpha_s)$ contributions to vector boson fusion have not yet been computed, although arguments exist that they will be small [6].

The calculation of the radiative corrections to the gluon fusion of Higgs bosons is in principle a two-loop calculation. However, in the limit $M_{top} \gg M_H$, an effective lagrangian similar to that of eq. (2.6) can be used and hence the gluonic radiative corrections can be found from a one-loop calculation. This will serve as a

valuable check of the complete two-loop calculation and should in principle give a reliable estimate of the size of these corrections in the relevant kinematic regime.

At this point it is important to discuss the spirit of the calculation. If the top quark is very heavy it will show up indirectly via its contribution to radiative corrections to various quantities such as the W and Z masses. Indeed, a global fit to existing data from electroweak processes requires $M_{\rm top} \lesssim 180$ GeV for the consistency of the standard model [7]. For the intermediate mass Higgs boson, say $M_{\rm H} \sim 100$ GeV, the $M_{\rm top} \gg M_{\rm H}$ limit may be a reasonable approximation. For a heavy Higgs boson, such as $M_{\rm H} \sim 1$ TeV, the $M_{\rm top} \to$ limit clearly is not valid. In this case, our results can be used to gauge the sensitivity of the Higgs boson production rate to new physics since any new heavy quarks will contribute to Higgs production from gluon fusion. For example, a doublet of heavy quarks which is degenerate in mass would not contribute to the ρ-parameter, but would contribute to the gluon fusion production of a Higgs boson.

3. Radiative corrections

3.1. THE SUBPROCESS $q\bar{q} \to gH$

The matrix element squared for the subprocess $q\bar{q} \to gH$ in the infinite top-quark mass limit is easily found from the Feynman diagram of fig. 3 using the effective lagrangian of eq. (2.6),

$$|M(q\bar{q} \to gH)|^2 = \frac{16}{9}\frac{\alpha_s^3}{\pi v^2}\frac{1}{s}\left(\frac{4\pi}{M_{\rm top}^2}\right)^{\epsilon}\Gamma(1+\epsilon)\left((u^2+t^2)-\epsilon(u+t)^2\right). \quad (3.1)$$

Since the cross section for this process is finite, it is straightforward to integrate over the phase space to find the spin- and color-averaged cross section,

$$\sigma(q\bar{q} \to gH) = \frac{1}{486\pi^2}\frac{\alpha_s^3}{v^2}\left(1-\frac{M_{\rm H}^2}{s}\right)^3. \quad (3.2)$$

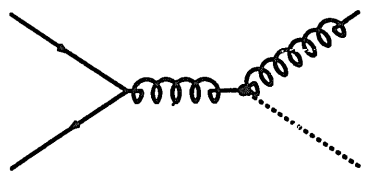

Fig. 3. Feynman diagram for the subprocess $q\bar{q} \to gH$. The dot represents the effective ggH vertex in the infinite top-quark mass limit.

3.2. THE SUBPROCESS qg → qH

The matrix element squared for the subprocess qg → qH can be found from crossing from that for $q\bar{q} \to gH$. We find

$$|M(qg \to qH)|^2 = -\frac{16}{9}\frac{\alpha_s^3}{\pi v^2}\frac{1}{t}\left(\frac{4\pi}{M_{top}^2}\right)^{\epsilon}\Gamma(1+\epsilon)\left((u^2+s^2)-\epsilon(u+s)^2\right). \quad (3.3)$$

The spin and color averages yield an additional factor of $1/96/(1-\epsilon)$. The cross section can be found by integrating with the N-dimensional phase space,

$$\sigma = \frac{1}{2s}\int |M|^2(\mathrm{PS}), \quad (3.4)$$

where a convenient parameterization of the phase space in N dimensions has been given in ref. [9]*,

$$(\mathrm{PS}) = \frac{1}{8\pi}\left(\frac{4\pi}{s}\right)^{\epsilon}\frac{1}{\Gamma(1-\epsilon)}(1-z)^{1-2\epsilon}\int_0^1 \omega^{-\epsilon}(1-\omega)^{-\epsilon}\,d\omega. \quad (3.5)$$

The scattering angle of the produced Higgs boson is $\cos\theta = 2\omega - 1$, which gives

$$t = -s(1-z)(1-\omega), \qquad u = -s(1-z)\omega, \quad (3.6)$$

where

$$z \equiv \frac{M_H^2}{s}. \quad (3.7)$$

The spin- and color-averaged cross section is found by performing the phase space integration over the matrix element squared, with the result

$$\sigma(qg \to qH) = \frac{\alpha_s^3}{864\pi^2 v^2}\left(\frac{4\pi}{s}\right)^{\epsilon}\left(\frac{4\pi}{M_{top}^2}\right)^{\epsilon}\Gamma^2(1+\epsilon)(1-z)^{-2\epsilon}$$
$$\times\left\{-\frac{1}{\epsilon}\left[1+(1-z)^2\right]-(1-z)\left(\frac{7-3z}{2}\right)\right\}. \quad (3.8)$$

* The calculation is similar to that of qg → qW of ref. [8]. Ref. [9] is a nice introduction to the necessary techniques.

We can relate the coefficient of the $1/\epsilon$ singularity to the Altarelli–Parisi splitting function [10],

$$P_{gq}(z) = \frac{4}{3}\left[\frac{1+(1-z)^2}{z}\right], \tag{3.9}$$

and use $(1-z)^{-2\epsilon} = 1 - 2\epsilon \log(1-z)$ to find

$$\sigma(qg \to qH) = \left(\frac{4\pi}{s}\right)^{\epsilon}\left(\frac{4\pi}{M_{top}^2}\right)^{\epsilon} \Gamma^2(1+\epsilon)\frac{\alpha_s^3}{1152\pi^2 v^2}$$

$$\times\left\{zP_{gq}(z)\left[-\frac{1}{\epsilon} + 2\log(1-z)\right] - \tfrac{2}{3}(1-z)(7-3z)\right\}. \tag{3.10}$$

The soft singularity can be factored into process-independent functions Γ_{ij} associated with the incoming parton legs. The physical cross section $\hat{\sigma}$ is then defined implicitly by the relation

$$\sigma_{ij}(s) = \sum_{i'j'} \int_0^1 dx_1\, dx_2\, \hat{\sigma}_{i'j'}(x_1 x_2 s)\Gamma_{j'j}(x_1)\Gamma_{i'i}(x_2), \tag{3.11}$$

where σ is the short-distance cross section which we have calculated and

$$\Gamma_{j'j}(x) \equiv \delta_{jj'}\delta(1-x) - \frac{\alpha_s}{2\pi}P_{j'j}(x)\frac{1}{\epsilon}(4\pi)^{\epsilon}\Gamma(1+\epsilon). \tag{3.12}$$

The association of the $(4\pi)^{\epsilon}\Gamma(1+\epsilon)$ with the $1/\epsilon$ singularity defines this to be the $\overline{\text{MS}}$ subtraction scheme. The factorization theorem [11] guarantees that $\hat{\sigma}$ is finite. Using eq. (2.7), our final answer for the physical cross section is then*

$$\hat{\sigma}(qg \to qH) = \frac{\alpha_s^3}{576\pi^2 v^2}\left\{-(1-z)\left(\frac{7-3z}{3}\right)\right.$$

$$\left. + \tfrac{1}{2}zP_{gq}(z)\left[1 + \log\left(\frac{M_H^2}{\mu^2}\frac{(1-z)^2}{z}\right)\right]\right\}. \tag{3.13}$$

To this order, the appropriate scale at which to evaluate σ_s is not determined. We will take $\alpha_s = \alpha_s(\mu)$, where the parameter μ is an arbitrary renormalization scale. The hadronic cross section is independent of μ to $O(\alpha_s^3)$.

* This agrees with ref. [2].

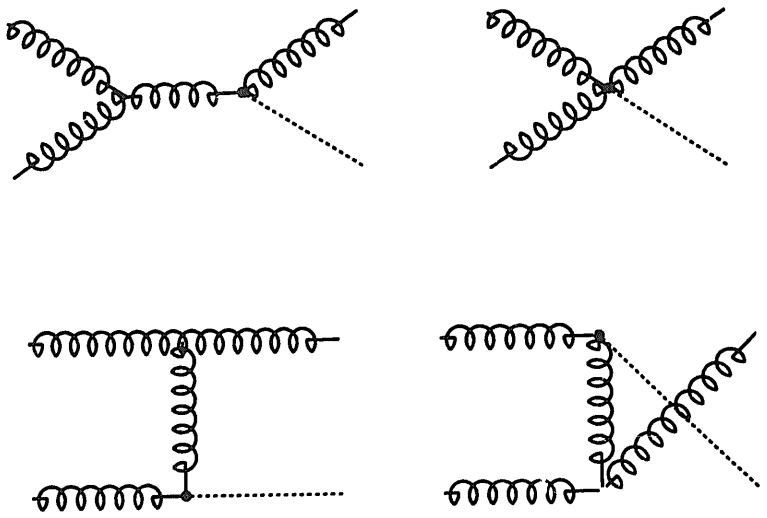

Fig. 4. Feynman diagrams contributing to the subprocess $gg \to gH$. The dot represents the effective gluon–Higgs coupling in the infinite top-quark mass limit.

The coefficient of the $\log \mu^2$ term in $\hat{\sigma}$ could have been predicted by renormalization group arguments,

$$\frac{\partial \hat{\sigma}(s)}{\partial \log \mu^2} = -\frac{\alpha_s}{2\pi} \int_0^1 dz' \sigma_0^{gg \to H}(z's) P_{gq}(z') . \tag{3.14}$$

3.3. THE SUBPROCESS $gg \to H$

To compute the radiative corrections to the inclusive production of the Higgs boson from gluon fusion we need both the real contributions from $gg \to gH$ and the virtual loop corrections from $gg \to H$. We being with the real contribution which is found from the Feynman diagrams of fig. 4. The matrix element squared for $gg \to gH$ has been computed by Ellis et al. [12] and by Hinchliffe and Novaes [13] in the $\epsilon \to 0$ limit. It is simplest to compute the amplitude for the process

$$H \to g^A(p^\mu) + g^B(q^\nu) + g^C(p'^\sigma) , \tag{3.15}$$

and then use crossing to obtain the amplitude for $gg \to Hg$. $ABC(\mu\nu\sigma)$ are the color (Lorentz indices). The amplitude can be written

$$\begin{aligned} M(H \to ggg) = {} & \mathscr{A}(p_A^\mu, q_B^\nu, p_C'^\sigma) + \mathscr{A}(p_A^\mu, p_C'^\sigma, q_B^\nu) \\ & + \mathscr{A}(q_B^\nu, p_C'^\sigma, p_A^\mu) + \mathscr{A}(q_B^\nu, p_A^\mu, p_C'^\sigma) \\ & + \mathscr{A}(p_C'^\sigma, p_A^\mu, q_B^\nu) + \mathscr{A}(p_C'^\sigma, q_B^\nu, p_A^\mu) . \end{aligned} \tag{3.16}$$

In the $M_{\rm top} \to \infty$ limit, the amplitude takes a simple form [12],

$$\mathscr{A}(p_A^\mu, q_B^\nu, p_C'^\sigma) = -\left(\frac{g_s^3}{24\pi^2 v}\right) f_{ABC}\left\{4\frac{p^\sigma}{t}\left(q^\mu p^\nu - \frac{s}{2}g^{\mu\nu}\right)\right.$$
$$\left. + \left[\frac{s^2+t^2+u^2-M_H^2}{st}\right]\left(p^\sigma g^{\mu\nu} + \frac{2}{3}\frac{p'^\mu p^\nu q^\sigma}{u}\right)\right\}, \quad (3.17)$$

where we define $s \equiv (p+q)^2$, $t \equiv (p+p')^2$ and $u \equiv (q+p')^2$. After crossing, s, t and u have their usual definitions.

Keeping terms to $O(\epsilon)$ we find the matrix element squared*,

$$|M(gg \to gH)|^2 = \frac{\alpha_s^3}{v^2}\left(\frac{32}{3\pi}\right)\left\{\left[\frac{M_H^8+s^4+t^4+u^4}{stu}\right](1-2\epsilon)\right.$$
$$\left. + \frac{\epsilon}{2}\left[\frac{(M_H^4+s^2+t^2+u^2)^2}{stu}\right]\right\}. \quad (3.18)$$

The spin and color averages yield an additional factor $1/256/(1-\epsilon)^2$.

Integrating over the N-dimensional phase space of eq. (3.5), it is straightforward to obtain the spin- and color-averaged cross section,

$$\sigma(gg \to gH)_{\rm real} = \frac{1}{576\pi^2}\frac{\alpha_s^3}{v^2}(1-z)^{-1-2\epsilon}\left(\frac{4\pi}{s}\right)^\epsilon \Gamma(1+\epsilon)\left(1-\frac{\pi^2\epsilon^2}{3}\right)$$
$$\times\left\{-\frac{3}{\epsilon}\left[1+z^4+(1-z)^4\right] - \tfrac{11}{2}(1-z)^4\right.$$
$$\left. -6(1-z+z^2)^2 - 6\epsilon\right\} + \ldots. \quad (3.19)$$

We have dropped terms proportional to $\epsilon(1-z)$ since they will give no contribution to the cross section.

The apparent singularity at $z=1$ is regulated by

$$(1-z)^{-1-2\epsilon} = \left(\frac{1}{1-z}\right)_+ - 2\epsilon\left(\frac{\log(1-z)}{1-z}\right)_+ - \frac{1}{2\epsilon}\delta(1-z). \quad (3.20)$$

* This of course agrees with the result of ref. [12] in the $\epsilon \to 0$ limit. We have consistently dropped an overall factor of $(4\pi/M_{\rm top}^2)^\epsilon \Gamma(1+\epsilon)$ in this subsection since it does not contribute to the end result.

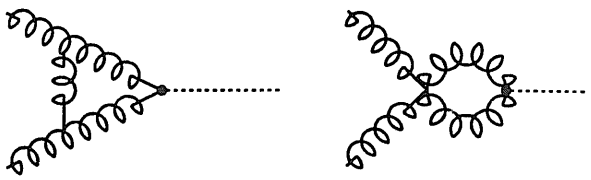

Fig. 5. Feynman diagrams giving virtual contributions to the subprocess gg → H in the infinite top-quark mass limit.

The plus distributions are defined in terms of the integrals

$$\int_0^1 \mathrm{d}x \frac{f(x)}{(x)_+} = \int_0^1 \frac{f(x)-f(0)}{x},$$

$$\int_0^1 f(x)\left(\frac{\log(x)}{x}\right)_+ = \int_0^1 \mathrm{d}x\,[f(x)-f(0)]\frac{\log(x)}{x}. \tag{3.21}$$

Combining eqs. (3.19) and (3.21), we find for the real contribution to the cross section

$$\sigma_{\mathrm{real}} = \frac{1}{576\pi^2}\frac{\alpha_s^3}{v^2}\left(\frac{4\pi}{s}\right)^{\epsilon}\Gamma(1+\epsilon)\left\{\left[\frac{3}{\epsilon^2}+\frac{3}{\epsilon}+3-\pi^2\right]\delta(1-z)\right.$$

$$-\frac{6z}{\epsilon}\left[\frac{z}{(1-z)_+}+\frac{1-z}{z}+z(1-z)\right]-\tfrac{11}{2}(1-z)^3$$

$$\left.+6\left[1+z^4+(1-z)^4\right]\left(\frac{\log(1-z)}{1-z}\right)_+-6\left[1-z+2z^2+\frac{z^4}{(1-z)_+}\right]\right\}. \tag{3.22}$$

We must now compute the virtual contributions to gg → H which are found from the diagrams of fig. 5. To $O(\alpha_s^2)$, the coupling of the Higgs boson to gluons in the $M_{\mathrm{top}} \to \infty$ limit can be found by noting that the Higgs boson couples to the trace of the energy–momentum tensor [4, 14]*,

$$\theta_\mu^\mu = \partial_\mu s^\mu = \frac{\beta(g_s)}{2g_s}G_{\mu\nu}G^{\mu\nu} + (1+\delta)M_{\mathrm{top}}\bar{t}t, \tag{3.23}$$

where s^μ is the scale current. The $(1+\delta)$ term arises from a subtlety in the use of the low-energy theorem [2, 15]. Since the Higgs coupling to heavy fermions is

* I thank the authors of ref. [2] for pointing out my omission of the $(1+\delta)$ term in the original version of this paper.

$M_{\rm top}(1+H/v)\bar{t}t$, the counterterm for the Higgs Yukawa coupling is fixed in terms of the fermion mass and wave function renormalization. We have $\delta = 2\alpha_s/\pi$. Hence, in the $M_{\rm top}\to\infty$ limit we find*

$$\mathscr{L}_{\rm eff} = \frac{H}{2v}\frac{\beta(g_s)}{g_s(1+\delta)}G_{\mu\nu}G^{\mu\nu}. \tag{3.24}$$

However, it is only the heavy fermions which contribute to β since the Hgg coupling results from heavy fermion loops only. To $O(\alpha_s^2)$, the heavy fermion contribution to the QCD β-function is [17]

$$\left.\frac{\beta(g_s)}{g_s}\right|_{\rm heavy\ fermions} = N_H\frac{\alpha_s}{2\pi}\left\{\frac{1}{3}+\frac{\alpha_s}{\pi}\frac{19}{12}\right\}, \tag{3.25}$$

and N_H is the number of heavy fermions. (We take $N_H = 1$ and consider only the top quark.)

The contribution to the cross section coming from virtual graphs is calculated using the effective lagrangian (3.24). After a straightforward computation we find the spin- and color-averaged cross section,

$$\sigma_{\rm virt} = \frac{\alpha_s^2}{576\pi v^2}z\delta(1-z)\left\{1+\frac{\alpha_s}{\pi}\left(\frac{4\pi}{M_H^2}\right)^{\epsilon}\Gamma(1+\epsilon)\right.$$
$$\left.\times\left[-\frac{3}{\epsilon^2}-\frac{3}{\epsilon}+\frac{5}{2}+2\pi^2\right]\right\}. \tag{3.26}$$

Note that when $\sigma_{\rm real}$ and $\sigma_{\rm virt}$ are combined the $1/\epsilon^2$ singularities cancel.

In order to regulate the $1/\epsilon$ singularities, we need to perform charge renormalization and to do the Altarelli–Parisi subtraction**. The charge renormalization is performed using the $\overline{\rm MS}$ subtraction scheme and the charge counterterm is (see e.g. ref. [18])

$$\sigma_{\rm ch} = (4Z_g)\sigma_0({\rm gg}\to{\rm H}), \tag{3.27}$$

where we must keep the $O(\epsilon)$ terms in σ_0 and

$$Z_g = -\frac{\alpha_s}{2\epsilon}(4\pi)^{\epsilon}\Gamma(1+\epsilon)b_0, \tag{3.28}$$

* It is important to note that it is impossible with this approach to generate any terms of $O(\log(M_{\rm top}^2/M_H^2))$. This is clear since the operator $(\beta/g)G^{\mu\nu}G_{\mu\nu}$ is scale invariant [16].

** We are working in an effective theory with no top quark (we have sent its mass off to infinity) so there is no wave-function renormalization and b_0 depends only on the light quarks.

where

$$b_0 = \frac{1}{4\pi}\left[11 - \tfrac{2}{3}n_{lf}\right] \tag{3.29}$$

and n_{lf} is the number of light quarks.

Finally, we must factor out the soft singularities as in eq. (3.11). This Altarelli–Parisi subtraction contributes a term to the physical cross section,

$$\sigma_{AP} = \sigma_0 \frac{\alpha_s}{\pi} P_{gg}(z) \frac{1}{\epsilon} \Gamma(1+\epsilon)(4\pi)^{\epsilon}, \tag{3.30}$$

where

$$P_{gg}(z) = 6\left[\frac{z}{(1-z)_+} + \frac{1-z}{z} + z(1-z)\right] + 2\pi b_0 \delta(1-z). \tag{3.31}$$

The physical cross section for $gg \to HX$ is now

$$\hat{\sigma} = \sigma_{real} + \sigma_{virt} + \sigma_{ch} + \sigma_{AP}. \tag{3.32}$$

It is convenient to write our final result as

$$\hat{\sigma}(gg \to HX) = \frac{\alpha_s^2(\mu)}{576\pi v^2}\left\{\delta(1-z) + \frac{\alpha_s(\mu)}{\pi}\left[h(z) + \bar{h}(z)\log\left(\frac{M_H^2}{\mu^2}\right)\right]\right\}. \tag{3.33}$$

We have then*

$$\begin{aligned} h(z) = {} & \delta(1-z)\left[\pi^2 + \tfrac{11}{2}\right] - \tfrac{11}{2}(1-z)^3 \\ & + 6\left(1 + z^4 + (1-z)^4\right)\left(\frac{\log(1-z)}{1-z}\right)_+ \\ & - 6\left[\frac{z^2}{(1-z)_+} + (1-z) + z^2(1-z)\right]\log(z), \\ \bar{h}(z) = {} & 6\left[\frac{z^2}{(1-z)_+} + (1-z) + z^2(1-z)\right]. \end{aligned} \tag{3.34}$$

(We remind the reader that $z = M_H^2/s$, where s is the gluon–gluon center-of-mass energy.) To be consistent we should use the one-loop β-function to determine the

* This agrees with ref. [2].

value of α_s in eq. (3.33). Note the large coefficient of $\delta(1-z)$ in $h(z)$. In sect. 4, we will see that this gives the dominant contribution to the $O(\alpha_s^3)$ corrections to Higgs production at both the SSC and LHC.

The coefficient of the logarithm, $\bar{h}(z)$, could have been predicted a priori from the renormalization group equation,

$$\frac{\partial\hat{\sigma}(s)}{\partial\log\mu^2} = -\frac{\alpha_s}{\pi}\int_0^1 dz'\,\sigma_0^{gg\to H}(z's)P_{gg}(z'), \tag{3.35}$$

where we note that to this order

$$\frac{\partial\alpha_s}{\partial\log\mu^2} = -b_0\alpha_s^2. \tag{3.36}$$

4. Results and structure functions

The parton level results of sect. 3 must be integrated with the quark and gluon distribution functions to find the physical cross sections. We begin by presenting our results using the EHLQ [19] structure functions with $\Lambda = 200$ MeV. We will comment later on the effects of changing the definition of the structure functions beyond the leading order and using different structure functions with different values of Λ.

In fig. 6 we show the lowest-order result of eq. (2.5) and the radiatively corrected result for $\sqrt{S} = 17$ TeV and 40 TeV. The radiatively corrected result includes all of the parton subprocesses. This figure uses the EHLQ structure functions with $\mu = M_H$. The effect of the radiative corrections is to raise the cross section by a factor of about 1.5 to 2. To assess the dependence on the choice of structure functions, we show in fig. 7 our result using the DFLM [20] structure functions with $\Lambda = 260$ MeV. For $M_H \lesssim 500$ GeV there is very little difference between the EHLQ and the DFLM curves. We remind the reader that our results are valid in the limit $M_{top} \gg M_H$. Since fits to electroweak data imply $M_{top} \lesssim 180$ GeV, in the absence of a new heavy quark our curves are probably valid only in the range $M_H \lesssim 200$ GeV. The numbers for heavier Higgs boson masses should be interpreted as being valid in the case where there is a heavy fourth-generation quark.

We would like to know how much of our result can be absorbed into a redefinition of the gluon structure function. At leading order, the parton structure functions, $f_i(x)$, are scheme independent. At the next-to-leading order, however, they depend on the scheme. In general we can write the transformation between two schemes as

$$f_i'(x) = f_i(x) + \frac{\alpha_s}{2\pi}\int_x^1 K_{ij}\left(\frac{x}{z}\right)f_j(z)\frac{dz}{z} + O(\alpha_s^2). \tag{4.1}$$

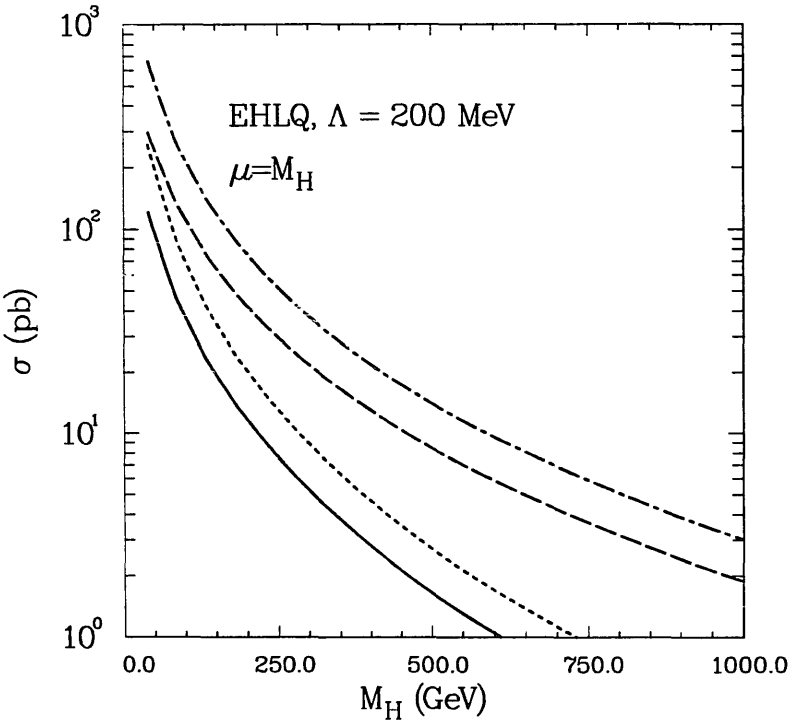

Fig. 6. Cross section for $pp \to H$ in the $M_{top} \to \infty$ limit using the EHLQ structure functions with $\Lambda = 200$ MeV and $\mu = M_H$. The solid (dashed) line is the lowest-order result, while the dotted (dot–dashed) line is the radiatively corrected result for $\sqrt{S} = 17$ TeV and 40 TeV, respectively.

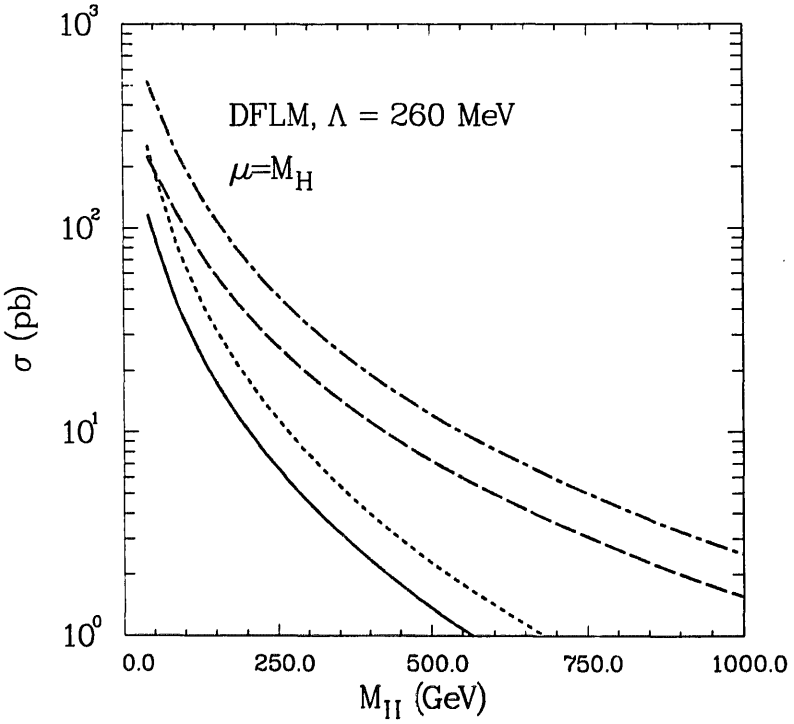

Fig. 7. Cross section for $pp \to H$ in the $M_{top} \to \infty$ limit using the DFLM structure functions with $\Lambda = 260$ MeV and $\mu = M_H$. The solid (dashed) line is the lowest-order result, while the dotted (dot–dashed) line is the radiatively corrected result for $\sqrt{S} = 17$ TeV and 40 TeV, respectively.

Physical quantities must be independent of the scheme used and so the short-distance cross sections in two different schemes must be related by

$$\sigma'_{ij}(s) = \sigma_{ij}(s) - \frac{\alpha_s}{2\pi}\sum_k \int_0^1 \sigma^0_{kj}(xs) K_{ki}(x)\,dx$$

$$- \frac{\alpha_s}{2\pi}\sum_l \int_0^1 \sigma^0_{il}(xs) K_{lj}(x)\,dx, \qquad (4.2)$$

where σ^0_{ij} is the lowest-order cross section for a process initiated by partons i and j.

For the case we are interested in, the relevant cross section is generated by the two-gluon initial state and we have to $O(\alpha_s^3)$

$$\sigma'_{gg}(s) = \sigma_{gg}(s) - \frac{\alpha_s}{\pi}\int_0^1 \sigma^0_{gg}(xs) K_{gg}(x)\,dx$$

$$= \sigma_{gg}(s) - \frac{\alpha_s^3}{576\pi^2 v^2} z K_{gg}(z),$$

$$\sigma'_{gq}(s) = \sigma_{gq}(s) - \frac{\alpha_s}{2\pi}\int_0^1 \sigma^0_{gg}(xs) K_{gq}(x)\,dx,$$

$$\sigma'_{q\bar{q}} = \sigma_{q\bar{q}}, \qquad (4.3)$$

where as usual $z \equiv M_H^2/s$.

We will use the definition of the structure functions beyond the leading order of ref. [21]. In this definition, the quark structure functions are defined such that F_2 as extracted from deep inelastic scattering is free from radiative corrections to $O(\alpha_s)$. With this definition we have [22]

$$K_{gg}(z) = -n_{lf}\left\{\left(z^2 + (1-z)^2\right)\log\left(\frac{1-z}{z}\right) + 6z(1-z)\right\}, \qquad (4.4)$$

where $n_{lf} = 5$ is the number of light flavors. The transformation of the gluon structure function is rather arbitrary and serves only to preserve the momentum sum rule to $O(\alpha_s)$. This is the appropriate transformation to use with the structure functions of ref. [20].

In fig. 8 we show the ratio of the radiatively corrected result for $pp \to H$ to the lowest-order result for $\sqrt{S} = 40$ TeV both with and without the transformation of eq. (4.4). The effect of this transformation is to absorb some of the radiative corrections into a redefinition of the gluon structure function. The numerical

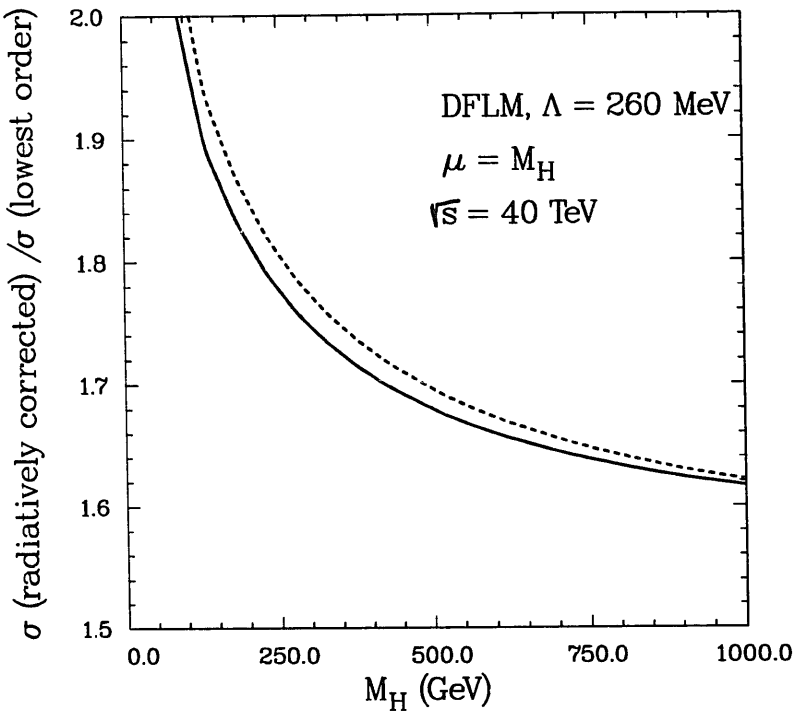

Fig. 8. Ratio of the radiatively corrected result for pp → H to the lowest-order result in the $M_{top} \to \infty$ limit. This figure uses the DFLM structure functions with $\Lambda = 260$ MeV and $\mu = M_H$ and has $\sqrt{S} = 40$ TeV. The solid line does not include the transformation of eq. (4.4), while the dotted line does.

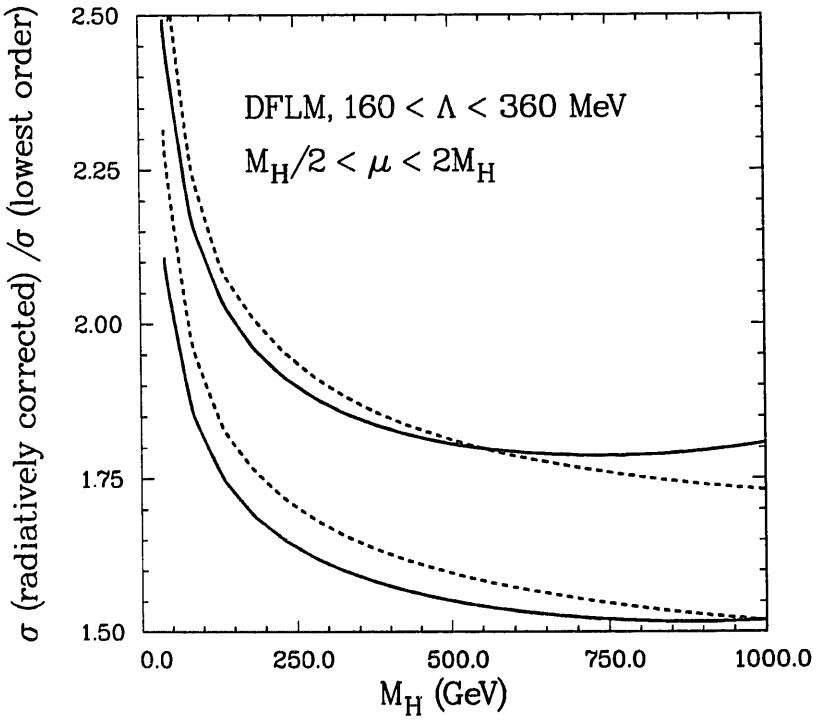

Fig. 9. Radiatively corrected cross sections for pp → H through the gluon fusion subprocess at the SSC (dotted lines) and the LHC (solid lines). The curves correspond to the range of values obtained when the renormalization scale μ is varied from $M_H/2$ to $2M_H$ and the QCD scale parameter is varied from $\Lambda = 160$ MeV to $\Lambda = 360$ MeV. These curves use the DFLM structure functions and include the transformation of eq. (4.4)

effects of this transformation can be seen however to be quite small. For $M_H \gtrsim 100$ GeV, the ratio of the radiatively corrected to the lowest-order cross section is approximately 1.7.

The effect of the radiative corrections is therefore to increase the cross section by a factor which is well approximated by a constant,

$$\sigma(gg \to H) \sim \sigma_0(gg \to H)\left[1 + \frac{\alpha_s}{\pi}\left(\pi^2 + \frac{11}{2}\right)\right]. \tag{4.5}$$

The cross section for Higgs boson production is quite sensitive to the choice of renormalization scale. For example, at the SSC for $M_H = 200$ GeV, the cross section increases by about 30% as μ is changed from $2M_H$ to $M_H/2$. We have attempted to quantify the uncertainty in the predictions from choice of renormalization scale and from choice of structure functions by showing in fig. 9 the range of values obtained by varying both μ and Λ through reasonable values. The lowest curve for each energy corresponds to the DFLM structure functions with $\Lambda = 160$ MeV and $\mu = 2M_H$.

5. Conclusion

We have computed the $O(\alpha_s^3)$ contributions to Higgs boson production at hadron colliders in the infinite top-quark mass limit. These corrections typically increase the lowest-order prediction by about a factor of 1.5 to 2. However, the results are sensitive to the choice of renormalization scale μ and to the choice of structure functions. It does seem clear, though, that the radiative corrections *increase* the cross section.

I thank W. Marciano, F. Paige and S. Willenbrock for valuable discussions. I am grateful to P. Zerwas for discussions of ref. [2].

References

[1] ALEPH Collab., Phys. Lett. B246 (1990) 306;
DELPHI Collab., Nucl. Phys. B342 (1990) 1;
L3 Collab., preprint L3-010 (1990);
OPAL Collab., CERN preprint EP-90-100 (1990)
[2] A. Djouadi, M. Spira and P. Zerwas, Aachen preprint PITHA 91/6, 1991
[3] F. Wilczek, Phys. Rev. Lett. 39 (1977) 1304;
J. Ellis, M.K. Gaillard, D.V. Nanopoulos and C.T. Sachrajda, Phys. Lett. B83 (1979) 339;
H. Georgi, S. Glashow, M. Machacek and D.V. Nanopoulos, Phys. Rev. Lett. 40 (1978) 692;
T. Rizzo, Phys. Rev. D22 (1980) 178
[4] A. Vainshtein, M. Voloshin, V. Zakharov and M. Shifman, Sov. J. Nucl. Phys. 30 (1979) 711;
A. Vainshtein, V. Zakharov and M. Shifman, Sov. Phys. Usp. 23 (1980) 429;
M. Voloshin, Sov. J. Nucl. Phys. 44 (1986) 478

[5] S. Dawson, Nucl. Phys. B249 (1985) 42;
G. Kane, W. Repko and W. Rolnick, Phys. Lett. B148 (1984) 367;
M. Chanowitz and M.K. Gaillard, Nucl. Phys. B261 (1985) 379
[6] S. Dawson, Phys. Lett. B217 (1989) 347
[7] U. Amaldi, Phys. Rev. D36 (1987) 1385
[8] G. Altarelli, R.K. Ellis and G. Martinelli, Nucl. Phys. B157 (1979) 461
[9] S. Willenbrock, BNL-43793, Lectures given at 1989 TASI Summer School
[10] G. Altarelli and G. Parisi, Nucl. Phys. B126 (1977) 298
[11] R.K. Ellis et al., Nucl. Phys. B152 (1979) 285
[12] R.K. Ellis, I. Hinchliffe, M. Soldate and J. Van der Bij, Nucl. Phys. B297 (1988) 221
[13] I. Hinchliffe and S. Novaes, Phys. Rev. D38 (1988) 3475
[14] J. Ellis, M.K. Gaillard and D.V. Nanopoulos, Nucl. Phys. B106 (1976) 292;
M.B. Voloshin, Yad. Fiz. 44 (1986) 738;
M. Shifman, Usp. Fiz. Nauk 157 (1989) 561
[15] E. Braaten and J. Leveille, Phys. Rev. D22 (1980) 715;
M. Drees and K. Hikasa, Phys. Lett. B240 (1990) 455;
S. Adler and W. Bardeen, Phys. Rev. D4 (1971) 3045
[16] H. Kluberg-Stern and J.-B. Zuber, Phys. Rev. D12 (1975) 467, 482, 3159
[17] W. Caswell, Phys. Rev. Lett. 33 (1974) 244;
D. Jones, Nucl. Phys. 75 (1974) 531
[18] R.K. Ellis, Lectures given at 1987 TASI Summer School
[19] E. Eichten et al., Rev. Mod. Phys. 56 (1984) 589
[20] M. Diemoz et al., Z. Phys. C39 (1988) 21;
J. Allaby et al., Phys. Lett. B197 (1987) 281
[21] G. Altarelli, R.K. Ellis and G. Martinelli, Nucl. Phys. B242 (1984) 120;
W. Furmanski and R. Petronzio, Z. Phys. C11 (1982) 293
[22] P. Nason, S. Dawson and R.K. Ellis, Nucl. Phys. B303 (1988) 607;
G. Altarelli, R.K. Ellis and G. Martinelli, Nucl. Phys. B157 (1979) 461